Janusz Czuchryj

Analysis of Fatigue Fractures in Elements Surfaced Using Various Methods and Tested in Relation to Complex Stresses

Abstract: Research-related fatigue tests at one stress level involved the simultaneous bending and torsion of elements made of steel C45, subjected to various surfacing methods and various post-surface heat treatment as well as having surfaced layers of various thicknesses. Fractures obtained in fatigue tests were subjected to visual and scanning microscopy-based analysis. The article presents the results of the above-named analysis and related concluding remarks.

Keywords: fatigue fractures, surfacing, steel C45, fatigue tests

DOI: *10.17729/ebis.2017.4/4*

Introduction

Fatigue service life tests aimed at comparing the workmanship of various elements are usually performed at one load level. In relation to elements (rollers) surfaced using various methods the adopted load level was that at which bending moment-triggered stresses σ_{gmax} amounted to 240 MPa, whereas torque moment-induced stresses τ_{smax}, amounted to 70 MPa. The stresses were determined through extensometric measurements. The lowest distortion-energy theory was used to calculate reduced stresses [1, 2]: $\sigma_z = \sqrt{\sigma_g^2 + \tau_S^2} =$

$= \sqrt{240^2 + 3 \cdot 70^2} = 268.887$ MPa ≈ 269 MPa.

At σ_z = 269 MPa, the fatigue service life tests were performed until the failure of the test elements. The obtained fatigue fractures were subjected to visual and scanning microscopy-based observation (3, 4, 5). The observation results were subjected to analysis and discussed below.

Shape, Dimensions and Quality of Test Elements

The complex load fatigue tests were performed on elements made of steel C45 (consistent with the requirements of PN-EN 10083-2), the shape and dimensions of which after surfacing and mechanical treatment are presented in Figure 1. The shape and dimensions of catch element result from the design of testing machine grips.

As can be seen in Figure 1, the elements were prepared for surfacing so that, after surfacing and machining, the working diameter would amount to 25 mm where the thickness of the surfaced layer would amount to g_1 = 1 mm and g_2 = 2 mm. The test elements were subjected to surfacing involving the use of process 111 and

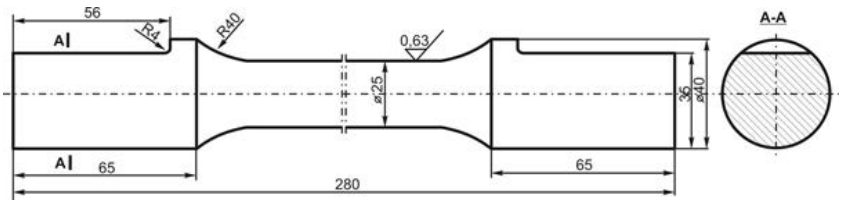

Fig. 1. Shape and dimensions of the test elements after surfacing and mechanical treatment

mgr inż. Janusz Czuchryj (MSc. Eng.) – Instytut Spawalnictwa, Non-destructive Testing Department

process 135 [6], consistent with definitions provided in PN-EN 4063, alternately along the longitudinal axes of the elements. The beginning and the end of each run extended (by approximately 15 mm) outside the cylindrical part of the element. After machining, the roughness of the elements amounted to R_a = 0.63 ÷ 0.32 μm. The elements were subjected to normalising annealing and toughening (Table 1).

Table 1. Test elements

Lot no.	Types of elements	Heat treatment	Thickness of surfaced layer
I II	Surfacing performed using process 111	Normalising annealing	1 mm 2 mm
III IV		Toughening	1 mm 2 mm
V VI	Surfacing performed using process 135	Normalising annealing	1 mm 2 mm
VII VIII		Toughening	1 mm 2 mm

The surfaced elements used in the fatigue tests, after being subjected to mechanical and heat treatment, were assessed using visual, penetrant and magnetic particle tests. The overlay weld surfaces did not reveal welding imperfections in the form of cracks. In some cases, single pores having a diameter of less than 1 mm and a depth (height) of approximately 0.5 mm were detected. The conducted tests did not enable the assessment of the quality of subsurface overlay weld layers.

To verify whether the heat treatment of the surfaced elements was performed properly, it was necessary to perform hardness measurements involving specimens cut in the plane passing across their longitudinal axis. The tests revealed that the elements subjected to toughening were characterised by higher hardness than those subjected to normalising. The test results confirmed that the heat treatment of the surfaced elements used in the fatigue tests was performed properly.

Tests of Fatigue Fractures

Fatigue cracks of the test elements were always formed in their surfaced part, at various areas along the length of the work segment. The fractures were subjected to visual inspection. The fatigue fractures of selected lot of the test elements are presented in Figures 2 ÷ 9. To demonstrate necessary details, the most interesting fragments of the fractures were magnified using photographic methods.

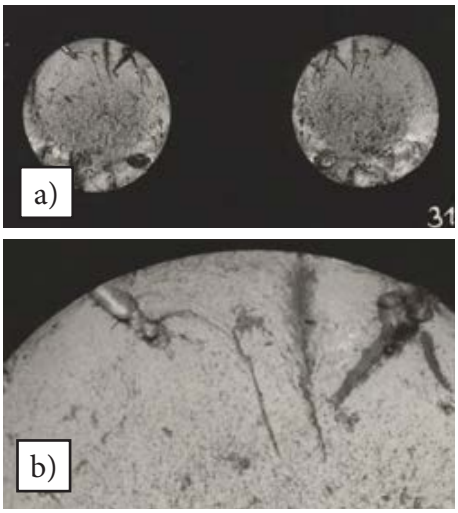

Fig. 2. Fatigue fracture of the element surfaced using process 111 and subjected to normalising annealing; lot II. a) natural size, b) 10x magnification of the fracture fragment with the imperfection on the left

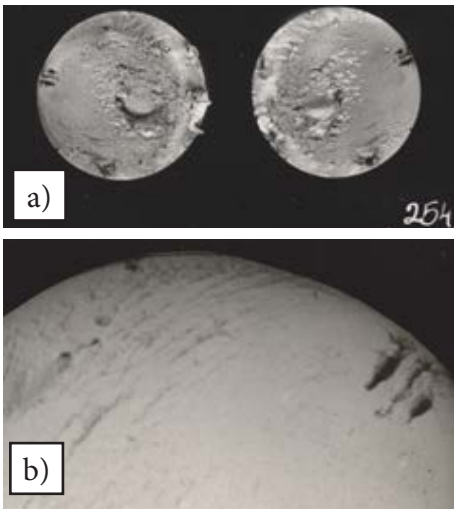

Fig. 3. Fatigue fracture of the element surfaced using process 111 and subjected to normalising annealing; lot II. a) natural size, b) 10x magnification of the fracture fragment with the imperfection on the right

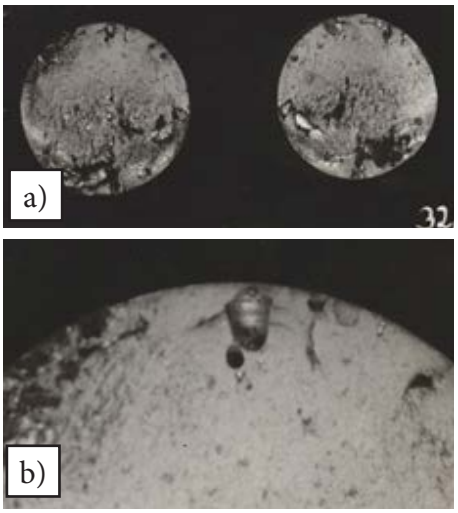

Fig. 4. Fatigue fracture of the element surfaced using process 111 and subjected to toughening; lot IV. a) natural size, b) 10x magnification of the fracture fragment with the imperfection on the left

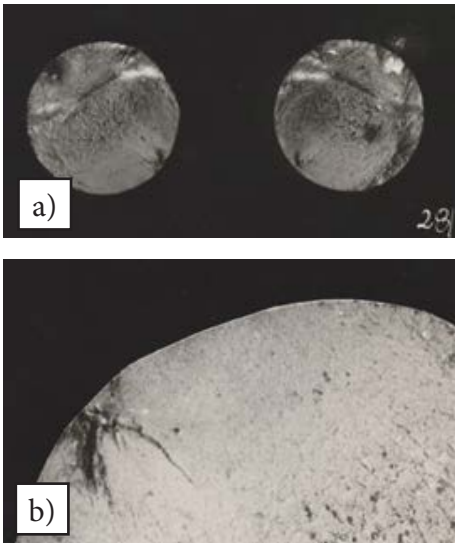

Fig. 5. Fatigue fracture of the element surfaced using process 111 and subjected to toughening; lot IV. a) natural size, b) 10x magnification of the fracture fragment with the imperfection on the left

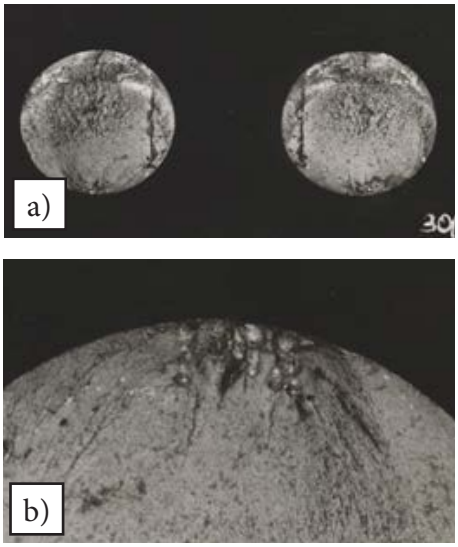

Fig. 6. Fatigue fracture of the element surfaced using process 135 and subjected to normalising annealing; lot VI. a) natural size, b) 10x magnification of the fracture fragment with the imperfection on the left

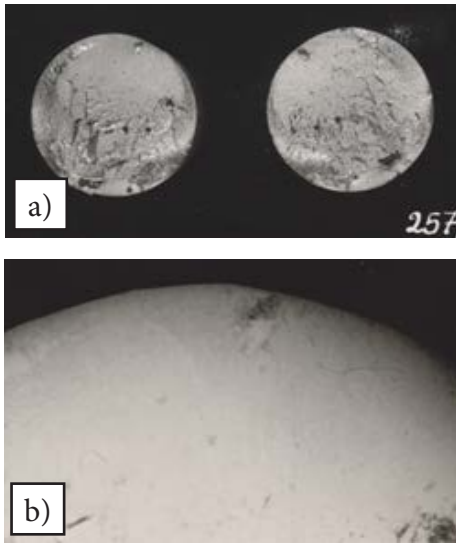

Fig. 7. Fatigue fracture of the element surfaced using process 135 and subjected to normalising annealing; lot VI. a) natural size, b) 10x magnification of the fracture fragment with the imperfection on the left

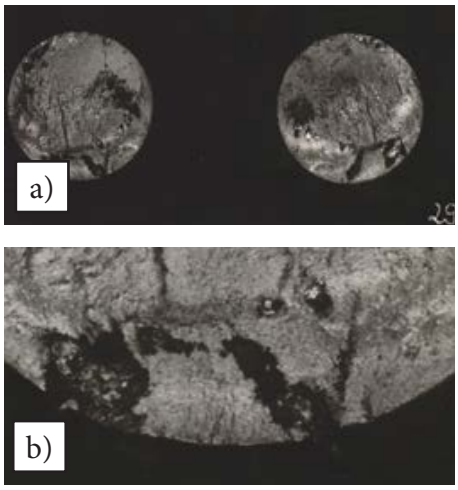

Fig. 8. Fatigue fracture of the element surfaced using process 135 and subjected to toughening; lot VIII. a) natural size, b) 10x magnification of the fracture fragment with the imperfection on the left

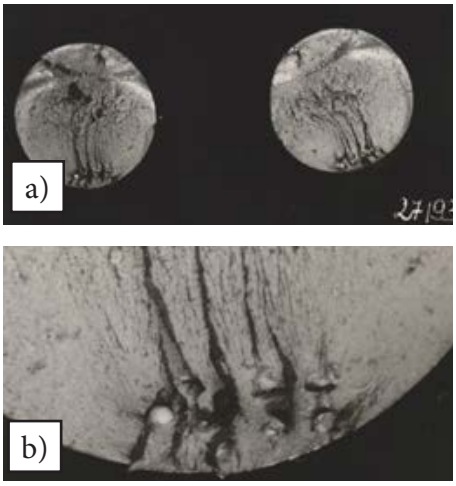

Fig. 9. Fatigue fracture of the element surfaced using process 135 and subjected to toughening; lot VIII. a) natural size, b) 10x magnification of the fracture fragment with the imperfection on the left

As can be seen in Figures 2-9, fatigue cracks were initiated at welding imperfections having the forms of slag and individual or grouped pores [7]. The above-named imperfections were always present in overlay welds and were ascribed to the improperly performed process. The planes of the fractures were perpendicular or nearly perpendicular in relation to the longitudinal axes of the elements with characteristic convexities and concavities on the surface. The above-presented fracture structure was characteristic of elements subjected to simultaneously performed bending and torsion [5].

The most important characteristics of the fracture fatigue zone include fatigue strips [5, 8], i.e. strips of consecutive cavities and convexities or strips with edges limited by the above-named cavities. Fatigue strips are marks representing cracks moving in every cycle and are perpendicular or nearly perpendicular in relation to the crack propagation direction, appear almost immediately when a crack is initiated and do not cover the entire surface of a fracture (Fig. 10).

The fatigue strips revealed on the fractures were used to determine the cracking rate $\Delta L/\Delta N$. Knowing the magnification of a fatigue fracture fragment with fatigue strips it was possible to calculate the distance between the lines (interline distance) ΔL. Assuming that each line corresponded to one changing load cycle, it was easy to calculate cracking rates of elements subjected to the tests (Table 2).

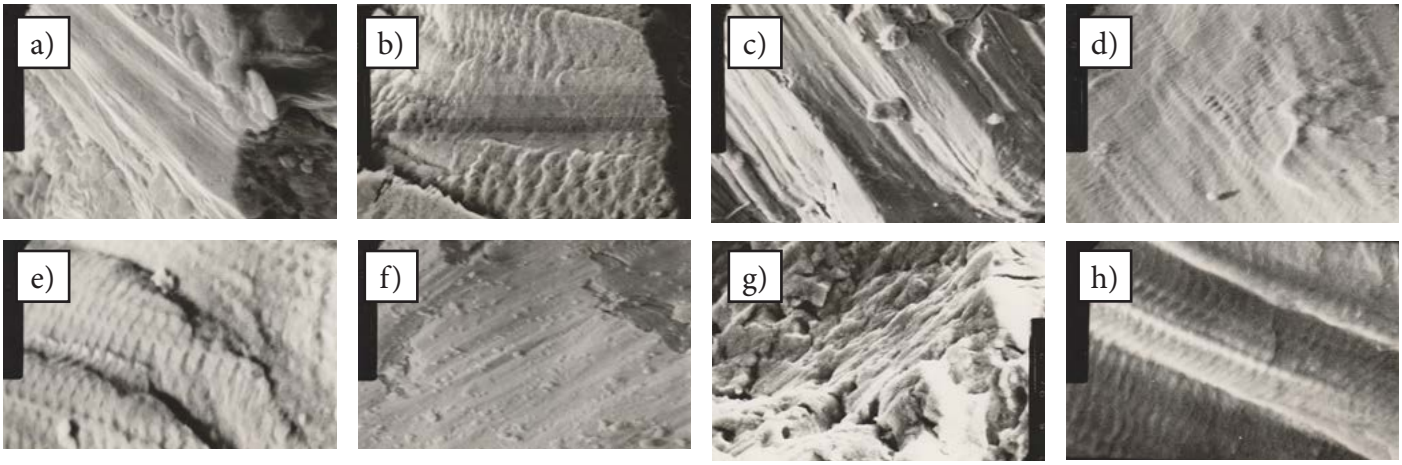

Fig. 10. Arrangements of fatigue strips on the segments of fractures triggered by simultaneously performed bending and torsion (magnified 3000 x) and after the number of load changes: a) N = 128200 cycles – lot I, b) N = 42000 cycles – lot II, c) N = 78800 cycles – lot III, d) N = 42300 cycles – lot IV, e) N = 69600 cycles – lot V, f) N = 106300 cycles – lot VI, g) N = 63100 cycles – lot VII, h) N = 36600 cycles – lot VIII

Table 2. Results of fatigue cracking rate measurements based on distances between fatigue strips

Lot no.	Types of elements	Heat treatment	Thickness of surfaced layer	Cracking rate $\Delta L/\Delta N$ mm/cycle	Average value of cracking rate $\Delta L/\Delta N$, mm/cycle	
I	Surfacing performed using process 111	Normalising annealing	1 mm	$0.75 \cdot 10^{-3}$	$1.01 \cdot 10^{-3}$	$0.97 \cdot 10^{-3}$
II			2 mm	$1.27 \cdot 10^{-3}$		
III		Toughening	1 mm	$0.87 \cdot 10^{-3}$	$0.93 \cdot 10^{-3}$	
IV			2 mm	$0.98 \cdot 10^{-3}$		
V	Surfacing performed using process 135	Normalising annealing	1 mm	$0.83 \cdot 10^{-3}$	$1.29 \cdot 10^{-3}$	$1.03 \cdot 10^{-3}$
VI			2 mm	$1.75 \cdot 10^{-3}$		
VII		Toughening	1 mm	$0.69 \cdot 10^{-3}$	$0.77 \cdot 10^{-3}$	
VIII			2 mm	$0.85 \cdot 10^{-3}$		

Table 2 reveals that the average cracking rate of the elements surfaced using covered electrodes (process 111) amounted to $0.97 \cdot 10^{-3}$ mm/cycle, whereas that of the elements surfaced in the shielding gas atmosphere (process 135) amounted to $1.03 \cdot 10^{-3}$ mm/cycle. As can be seen, the cracking rate of the elements subjected to surfacing performed using process 135 was higher than that of the subjected to surfacing performed using process 111.

Analysis of Test Results and Conclusions

Most moving elements of machinery, equipment and vehicles are exposed to complex and changeable loads. One of the methods enabling the extended use of such elements is surfacing. The fatigue tests including the simultaneous application of bending and torsion involved elements surfaced using various surfacing techniques, having various thicknesses of surfaced layers and subjected to various post-surface heat treatment (Table 1). The tests were performed at one stress level. The analysis involved fractures of surfaced elements obtained after fatigue tests.

The elements used in the fatigue tests were subjected to surfacing involving the use of processes 111 and 135, i.e. methods commonly used in industrial practice and characterised by proper technological development.

The surfaced elements were subjected to non-destructive tests including visual tests, penetrant tests and magnetic particle tests. The visual, penetrant and magnetic particle tests did not reveal the presence of welding imperfections

in the form of cracks on the overlay weld surfaces, which confirmed that the surfacing of the test elements was performed properly.

To verify whether the heat treatment of the surfaced elements was performed properly, it was necessary to perform hardness measurements. The tests revealed that in each case the elements subjected to toughening were characterised by higher hardness than those subjected to normalising. The hardness measurement results met related expectations and confirmed that the heat treatment of the surfaced test elements was performed properly.

In all of the surfaced elements, fatigue cracks were initiated at the welding imperfections (individual or grouped pores or slag) located in the overlay welds (Fig. 2÷9). The presence of welding imperfections in layers surfaced using processes 111 and 135 is unavoidable and should be accepted. In many cases, such imperfections cannot be detected using the primary non-destructive tests. However, the use of special methods is problematic and often costly.

The fractographic tests revealed the presence of regular fatigue strips on the surface of the fractions (Fig. 10). The strips reflected the consecutive location of the crack face and were perpendicular or nearly perpendicular in relation to the direction of crack propagation. The strips appeared nearly immediately when the crack was initiated and did not cover the entire surface of the fracture. The surface of the strips revealed the traces of edges, corrugations and smaller strips, which proved the complexity of cracking during the simultaneous bending and twisting of elements. The fatigue strips revealed on the fractures were used to determine the cracking rate $\Delta L/\Delta N$ (Table 2).

The performed measurements revealed that the average cracking rate of the elements surfaced using process 111 amounted to $0.97 \cdot 10^{-3}$ mm/cycle, whereas that of the elements surfaced using process 135 amounted to $1.03 \cdot 10^{-3}$ mm/cycle. As can be seen, the cracking rate of the elements subjected to gas-shielded surfacing was higher than that of the elements subjected to surfacing performed using covered electrodes. The above-named result was justified as the removal of slag in process 135 is difficult due to the fact that layers surfaced using the above-named method contain a greater number of crack initiators than layers surfaced using covered electrodes. For this reason, the likelihood of the failure of elements surfaced using process 135 is higher.

The situation was similar in cases of 1 mm and 2 mm thick surfaced layers. In each case, the cracking rate of the elements having the 2 mm thick overlay weld was higher than that of the elements having the 1 mm thick overlay weld (e.g. the cracking rate of the elements of lot II amounted to $1.27 \cdot 10^{-3}$ mm/cycle, whereas that the elements of lot I amounted to $0.75 \cdot 10^{-3}$ mm/cycle). The foregoing can be ascribed to the fact that an increase in the thickness of a surfaced layer entails an increase in the number of welding imperfections present in that layer leading to an increase in the number of potential crack initiators and an increase in the statistical probability of crack initiation. As can be see, cracking rates of elements with thick overlay welds tends to be higher than those of elements with thin overlay welds.

In addition, as can be seen in Table 2, the average cracking rate of the elements subjected to surfacing and normalising annealing was higher than that of the elements subjected to surfacing and toughening. For instance, the average cracking rate of the normalised elements of lots V and VI amounted to $1.29 \cdot 10^{-3}$ mm/cycle, whereas that of the toughened elements of lots VII and VIII amounted to $0.77 \cdot 10^{-3}$ mm/cycle. As can be seen, the hardening of the base material and overlay weld material structure favourably affected the initiation of fatigue cracking, significantly delaying the above-named process.

The performed analysis led to the conclusion that the service life of surfaced elements is affected by the period of fatigue crack initiation and not by that of fatigue crack propagation.

The performed tests enabled the formulation of the following conclusions:

1. The planes of the fatigue fractures of surfaced elements subjected to bending and torsion at the same time were perpendicular or nearly perpendicular to their longitudinal axes.
2. The fatigue fractures of surfaced elements were initiated at the welding imperfections present individually or in groups in the surfaced layers.
3. The cracking rate of surfaced elements determined on the basis of distances between fatigue strips depended on surfacing methods, thicknesses of surfaced layers and the heat treatment of these elements.
4. The service life of surfaced elements was affected by the period of fatigue crack initiation and not by that of fatigue crack propagation

References:

[1] Bodnar A.: *Wytrzymałość materiałów*. KWM IBM PK, Kraków, 2004.

[2] Kurowski R., Niezgodziński M.: *Wytrzymałość materiałów*. Ed. IX edited. Państwowe Wydawnictwo Naukowe, Warszawa, 1970.

[3] Czuchryj J., Sikora S.. *Metody i techniki badań nieniszczących złączy spawanych*. Ed. I. Wydawnictwo Instytutu Spawalnictwa, Gliwice, 2014.

[4] Słania J., Staniszewski K.: *Próba łamania złączy spawanych. Atlas przełomów*. Agenda wydawnicza SIMP, Redakcja Przegląd Spawalnictwa. Warszawa, 2014.

[5] Kocańda S.: *Zmęczeniowe zniszczenie metali*. Wydawnictwa Naukowo–Techniczne, Warszawa, 1978.

[6] Rjabcew I.A., Sjenczenkow I.K., Turyk E.: *Napławka, matieriały, tiechnołogii, matiematiczeskoje modielirowanije*. Wydawnictwo Politechniki Śląskiej, Gliwice, 2015.

[7] Czuchryj J., Sikora S.: *Niezgodności spawalnicze w złączach spawanych z metali i termoplastycznych tworzyw sztucznych*. Ed. I. Wydawnictwo Instytutu Spawalnictwa, Gliwice, 2016.

[8] Robakowski T., Czuchryj J.: Torsionswechselfestigkeit von Reibschweissverbindungen aus Stahl 45. Schweisstechnik, 1984, no. 10, pp. 473-474.

Reference standards:

- PN-EN 10083-2: *Steels for quenching and tempering. Part 2: Technical delivery conditions for non alloy steels*
- PN-EN ISO 4063: *Welding and allied processes – Nomenclature of processes and reference numbers*